its theoretical convergence rate only for $E_1 \geq 10^{-4}$. Below this value the error is dominated by the grid nonuniformity [see Eq. (5)], and each scheme shows similar behavior. For a course grid ($N = 32$) the change occurs at a higher value of E_1. E_2 also shows similar behavior (not shown here).

Another property of the approximate operators is the behavior of the error at large w. This is important because it determines the range of spatial scales that can be resolved by the numerical scheme.[5] In Tables 2 and 3 the resolved fraction for 10% error in w' and w'' is listed, respectively, for the numerical schemes tested. It can clearly be seen that for stretched grids the spectral-like accuracy of the compact finite difference schemes has not been maintained. For all schemes tested, the magnitude of errors is increased substantially. It is also found that the higher the scheme order, the larger the error grows. In COM6 and PADE the accuracy decreases substantially at $\gamma = 3$. However, grid nonuniformity decreases the 10% resolved fraction of CEN2 only marginally. Therefore, as the grid nonuniformity increases ($\gamma = 3$) the benefit of using higher-order schemes almost disappears. Unlike the higher-order schemes, CEN2 error is not greatly affected by grid nonuniformity.

IV. Conclusions

The accuracy of higher-order finite difference schemes on a nonuniform grid is investigated. Four finite difference schemes that are widely used in DNS and LES are considered: a sixth-order compact scheme (COM6), the standard Padé scheme (PADE), the fourth-order central difference (CEN4), and the second-order central difference (CEN2). Two types of nonuniform grid are tested: hyperbolic-sine and hyperbolic-tangent grids. The grid quality has stronger effects on the higher-order compact schemes than on CEN4 and CEN2. It is found that CEN2 scheme is highly insensitive to grid quality, justifying its popularity in engineering computational fluid dynamics. The accuracy deterioration of higher-order compact schemes with low grid density is observed. Unlike CEN2, such schemes use broad information to evaluate derivatives. Consequently, higher-order schemes are more sensitive to grid quality. Although we considered two types of nonuniform grid, the findings of the present work can be generally extended to nonuniform grids where we can find a smooth mapping function.

Acknowledgment

The support of the Engineering and Physical Sciences Research Council of the United Kingdom under Grant GR/N05581 is gratefully acknowledged.

References

[1]Lele, S. K., "Compact Finite Difference Schemes with Spectral-Like Resolution," *Journal of Computational Physics*, Vol. 103, 1992, pp. 16–42.

[2]Sandham, N. D., and Reynolds, W. C., "Three Dimensional Simulations of Large Eddies in the Compressible Mixing Layer," *Journal of Fluid Mechanics*, Vol. 224, 1991, p. 133.

[3]Chung, Y. M., Luo, K. H., and Sandham, N. D., "Direct Numerical Simulation of an Impinging Jet," *International Journal of Heat and Fluid Flow*, Vol. 23, No. 5, 2002, pp. 592–600.

[4]Kim, J. W., and Lee, D. J., "Optimized Compact Finite Difference Schemes with Maximum Resolution," *AIAA Journal*, Vol. 34, No. 5, 1996, pp. 887–893.

[5]Kwok, W. Y., Moser, R. D., and Jiménez, J., "A Critical Evaluation of the Resolution Properties of B-Spline and Compact Finite Difference Methods," *Journal of Computational Physics*, Vol. 174, 2001, pp. 510–551.

[6]Carpenter, M. H., Gottlieb, D., and Abarbanel, S., "The Stability of Numerical Boundary Treatments for Compact High-Order Finite-Difference Schemes," *Journal of Computational Physics*, Vol. 108, 1993, p. 272.

[7]Adams, N. A., "Direct Numerical Simulation of Turbulent Compression Ramp Flow," *Theoretical and Computational Fluid Dynamics*, Vol. 12, 1998, pp. 109–129.

[8]Kim, J., Moin, P., and Moser, M., "Turbulent Statistics in Fully Developed Channel Flow at Low Reynolds Number," *Journal of Fluid Mechanics*, Vol. 177, 1987, p. 133.

[9]Chung, Y. M., and Sung, H. J., "Initial Relaxation of Spatially Evolving Turbulent Channel Flow with Blowing and Suction," *AIAA Journal*, Vol. 39, No. 11, 2001, pp. 2091–2099.

[10]Yang, K. S., and Ferziger, J. H., "Large-Eddy Simulation of Turbulent Obstacle Flow Using a Dynamic Subgrid-Scale Model," *AIAA Journal*, Vol. 31, 1993, p. 1406.

R. M. C. So
Associate Editor

Vibration–Dissociation Coupling Model for Hypersonic Blunt-Body Flow

Eswar Josyula*
U.S. Air Force Research Laboratory, Wright–Patterson Air Force Base, Ohio 45433
and
William F. Bailey†
U.S. Air Force Institute of Technology, Wright–Patterson Air Force Base, Ohio 45433

Nomenclature

k	=	Boltzmann constant
L	=	last vibrational level
M	=	Mach number, molecular weight
T	=	translational temperature
T_v	=	vibrational temperature for which population densities correspond to a Boltzmann distribution
v, w	=	vibrational quantum numbers
x, y	=	Cartesian coordinates
Γ_v	=	equilibrium fractional population in state v
ϵ	=	quantum level energy
ρ_s	=	density of species s
ρ_v	=	state density in the vth vibrational level
φ_L	=	deviation of last vibrational level, the dissociating state
φ_v	=	deviation of quasisteady distribution from an equilibrium Boltzmann distribution

Subscripts

i, j	=	species indices in quantum levels v, w
s	=	species O_2, N_2, O, N
v	=	vibrational level

Introduction

THE kinetics of thermal dissociation has long been a topic of theoretical research because of the difficulty of reconciling the measured rates. Current kinetic processes associated with reconciling the disparity include depletion effects from the upper vibrational levels and possible effects of rotational energy on the dissociation mechanism. Early attempts by Hammerling et al.[1] to model vibration–dissociation coupling (CVD) used a simple harmonic oscillator assumption for the vibrational energy resulting in the vibrational population relaxing through a sequence of Boltzmann distributions. The coupled vibration–dissociation (CVDV) model of Treanor and Marrone[2] extended the CVD model to account for

Presented as Paper 2001-2733 at the AIAA 32nd Plasmadynamics and Lasers Conference, Anaheim, CA, 11–14 June 2001; received 3 October 2001; revision received 10 April 2003; accepted for publication 21 April 2003.

*Research Aerospace Engineer, AFRL/VAAC, 2210 Eighth Street. Associate Fellow AIAA.
†Associate Professor, AFIT/ENP, 2950 P Street.

the removal of vibrational energy by dissociation and favored the weak bias mechanism later, to consistently account for the incubation time. Marrone[3] introduced an additional factor in this model to make the probability of dissociation an increasing function of the vibrational quantum number. Based partly on these studies, an empirical two-temperature vibration–dissociation model was proposed by Park.[4] Its ease of implementation in numerical codes and good agreement with experimental data for radiative energy flux[5] made the model very popular for vibration–dissociation coupling in hypersonic aerodynamic flows. In some recent studies, however, the treatment of vibration–dissociation coupling using Park's two-temperature dissociation model yielded up to 20% lower shock-standoff distances compared to data for blunt-body flows (see Refs. 6 and 7) in the Mach-number range of 11–16.

In the work of Josyula and Bailey[7] the collisional approach to dissociation was adapted in the study of reactive, hypersonic flow past a blunt body. In this study the vibrational master equations were coupled to fluid dynamic equations, and vibration–translation (V-T) processes were considered in evaluating the depletion effects caused by dissociation from the last quantum level for diatomic nitrogen. The current work presents the vibration–dissociation coupling model by evaluating the depletion effects in oxygen and makes direct comparisons with experiment. By restricting vibrational exchanges to V-T transfers, an upper bound on the population depletion in the vibration manifold and consequent dissociation rate reduction is established for hypersonic blunt body flow conditions.

Analysis

The governing equations of mass, momentum, and energy of the hypersonic flow are the Navier–Stokes equations with source term for the chemical species as described in Ref. 8. The vibrational energy for the diatomic species of oxygen and nitrogen is calculated using the Landau–Teller method.[9] However, the vibrational–dissociation coupling model for oxgyen dissociation adopts an anharmonic oscillator description with vibrational energy given by

$$e_{\mathrm{vib}_s} = \sum_{i=1,2,..} \frac{\rho_i}{\rho_s}\epsilon_i \tag{1}$$

Here, ρ_i/ρ_s is the fractional population of the ith vibrational level and ϵ_i the quantum level energy given by the third-order approximating formula:

$$\epsilon_i/hc = \omega_e\left(i-\tfrac{1}{2}\right) - \omega_e x_e\left(i-\tfrac{1}{2}\right)^2 + \omega_e y_e\left(i-\tfrac{1}{2}\right)^3 \qquad i = 1, 2, \ldots L+1 \tag{2}$$

where h is the Planck's constant and c is the speed of light. The spectroscopic constants for the O_2 molecules are given by[10] $\omega_e = 1580.19\,\mathrm{cm}^{-1}$, $\omega_e x_e = 11.98\,\mathrm{cm}^{-1}$, and $\omega_e y_e = 0.04740\,\mathrm{cm}^{-1}$. When $i = 37$, the value of energy exceeds the O_2 dissociation energy, 5.12 eV.

Dissociation Kinetics

For the present simulations of an airflow past the blunt body, the maximum temperature of the shock was below 5000 K. Under these circumstances the dominant dissociation reaction is $O_2 + M \rightleftharpoons 2O + M$. The equilibrium reaction rates and equilibrium constants were taken from the work of Park.[11] Chemical source terms consisted of dissociation rates determined from the Arrhenius equation and recombination rates, derived from the law of mass action. The equilibrium dissociation rates for oxygen given in Ref. 11 were modified by the present vibration–dissociation coupling model to yield the nonequilibrium dissociation rates.

Vibration–Dissociation Coupling

This section presents the kinetic equations describing the dissociative-relaxation coupling by considering the balance equations for the number of particles in each vibrational level. The approach is an extension of the original formulation of Osipov and Stupochenko.[12] The state-specific rate equations for the vibrational states are written as

$$\dot{\rho}_v = \sum_{v'}\left[k_{\mathrm{VT}}(v' \to v)\rho_{v'}\rho_{\mathrm{O}_2} - k_{\mathrm{VT}}(v \to v')\rho_v\rho_{\mathrm{O}_2}\right] + k_{rv}\rho_{\mathrm{O}}^2\rho_{\mathrm{O}_2} - k_{\mathrm{dv}}\rho_v\rho_{\mathrm{O}_2}, \qquad v = 0, 1, \ldots L \tag{3}$$

$$\frac{1}{2}\dot{\rho}_{\mathrm{O}} = \sum_{v=0}^{L} k_{\mathrm{dv}}\rho_v\rho_{\mathrm{O}_2} - \sum_{v=0}^{L} k_{\mathrm{rn}}\rho_{\mathrm{O}}^2\rho_{\mathrm{O}_2} \tag{4}$$

Here ρ_v is the mass density in level v; $k_{v' \to v}$ and $k_{v \to v'}$ are the V-T rate coefficients for vibrational transitions to occur from $v' \to v$ and $v \to v'$; k_{dv} and k_{rv} are the rate constants for dissociation/recombination in transition from/to vibrational state v to/from continuum; ρ_{O_2} is the total mass density of oxygen; and L is the last discrete vibrational level of the molecule. Note that

$$\sum_{v=0}^{L}\rho_v = \rho_{\mathrm{O}_2}$$

The mass density in vibrational state v is then given by

$$\rho_v(t) = \rho_v^{(0)}(t)(1+\varphi_v) \tag{5}$$

The deviation coefficient φ_v in the simplest case of single-quantum energy transitions and dissociation restricted to the last discrete vibrational level is given by

$$\varphi_v = \frac{\tilde{k}_{\mathrm{diss}}}{\rho_{\mathrm{O}_2}^2}\sum_{i=1}^{v}\frac{1}{k_{i-1,i}\Gamma_{i-1}}\left(\sum_{j=0}^{i-1}\Gamma_j\right) + \varphi_0 \tag{6}$$

Here $\tilde{k}_{\mathrm{diss}}$ is the global rate of the dissociation reaction. The Γ_v term is given by

$$\Gamma_v = \frac{\exp(-\epsilon_v/kT)}{\sum_{v'=0}^{L}\exp(-\epsilon_{v'}/kT)} \tag{7}$$

The φ_0 term, the deviation for the ground vibrational level, is determined from the normalization condition for Eq. (5):

$$\sum_{v=0}^{L}\rho_v^{(0)}\varphi_v = 0$$

From this condition it follows that

$$-\varphi_0 = \frac{1}{\rho_{\mathrm{O}_2}}\sum_{v=1}^{L}\rho_v^{(0)}\tilde{\varphi}_v \tag{8}$$

where $\tilde{\varphi}_v = \varphi_v - \varphi_0$.

Conditions of Numerical Simulation

Simulations were performed on an axisymmetric blunt-body flow to study the effect of vibration–dissociation coupling with special attention to the rate of depletion. This particular assessment was motivated by the inability of the Park two-temperature dissociation model to predict the shock-standoff distance correctly.[6,7]

The blunt body had a hemisphere nose forebody of radius 0.007 m. For a Mach 11.18 airflow the freestream equilibrium temperature was 293 K and the pressure 1200 Pa. The numerical algorithm employed to solve the coupled set of equations is the Roe flux-difference method described in Ref. 13. The upstream and far-field boundary conditions were prescribed as the undisturbed freestream values. At the downstream boundary the no-change condition was imposed for the predominantly supersonic flowfield. On the body surface $n \cdot \boldsymbol{u}$ is zero, where n is the surface normal vector. The finite volume formulation of the present work allows fluxes at the singular line of symmetry to be set to zero because the control surface of the elementary cell at the axis of symmetry merges to a point. Initial conditions were set to freestream uniform flow conditions.

Results and Discussion

The physics of the state-to-state vibration–dissociation coupling model and its effect on hypersonic blunt-body flow predictions are presented next.

Vibration–Dissociation Coupling

The ratio of nonequilibrium to equilibrium population in the last vibrational state $1 + \varphi_L$ is shown in Fig. 1. The departure from equilibrium decreases with temperature. At lower gas temperatures in the flowfield (for which oxygen dissociation takes place), the effect of depletion of vibrational population can be significant with the nonequilibrium dissociation rate being reduced by this factor. The depletion was calculated considering dissociation to occur only from the last level. In addition, the depletion analysis was restricted to include only V-T exchanges and only V-T exchanges with parent O_2 molecule. The accelerating influence of vibration–vibration exchanges and V-T exchanges with the dissociation products was neglected. Taken together, these restrictions establish an upper bound on the depletion in the vibration manifold.

Comparison with Experiment

The experimental data and computational results of shock-standoff distance are in Fig. 2. The computations neglecting depletion effects, presented here for comparison, were discussed in an earlier paper.[7] The traces corresponding to the idealized conditions of equilibrium and $\gamma = \frac{7}{5}$ (frozen flow) are also presented for reference. For velocities less than 3000 m/s, the shock-standoff distances are consistent with frozen flow conditions, and vibration–dissociation models, without depletion effects, are deemed adequate. However at higher flow velocitiess discussed in the earlier paper,[14] simulations failing to account for the depletion deviate about 20% from experiment. This deviation is attributable to the excessive dissociation rates predicted by the Park two-temperature dissociation model. In contrast, the present computation, which includes the depletion effects, corrects this overestimate of the rates and predicts a reduced shock-standoff distance that is more consistent with the experimental data (Fig. 2).

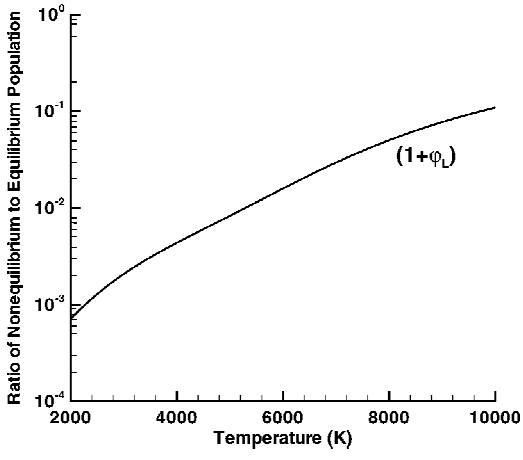

Fig. 1 Nonequilibrium-to-equilibrium population ratio in the last vibrational state for Park's dissociation model.

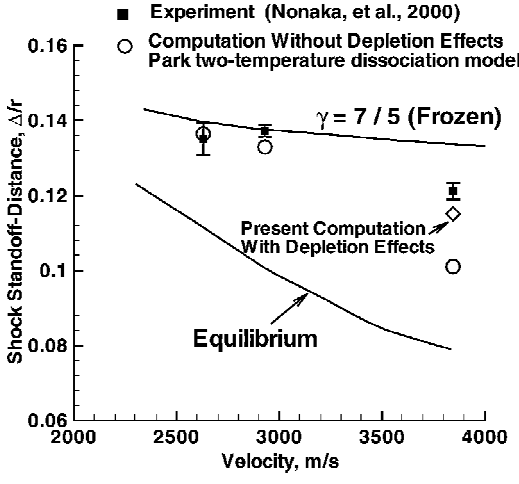

Fig. 2 Comparison of shock-standoff distances for flow past a blunt body: medium = air, test condition radius = 0.007 m.

Conclusions

A computational study was conducted for nonequilibrium hypersonic flow past a hemisphere cylinder. A new vibration–dissociation coupling model was implemented to assess the extent of the depletion of vibrational population and dissociation rate reduction. The reduction in the equilibrium dissociation rates of oxygen in the temperature range of 2000–10,000 K was quantified. In the lower temperature range the rates were substantially reduced compared to those of Park's two-temperature dissociation model, but the rates were consistent with Park's rates at the high end. For temperature range of 2000–6000 K, where oxygen dissociation is important in hypersonic flight, the rate reduction was more than two orders of magnitude. For a Mach 11.18 airflow past a blunt body, the Park two-temperature dissociation model underpredicts experimental shock-standoff distance by 20%. The present vibration–dissociation model yields results more consistent with the data and provides an upper bound on depletion in the vibrational manifold.

References

[1]Hammerling, P., Teare, J., and Kivel, B., "Theory of Radiation from Luminous Shock Waves in Nitrogen," *Physics of Fluids*, Vol. 2, No. 4, 1959, pp. 422–426.

[2]Treanor, C., and Marrone, P., "Effect of Dissociation on the Rate of Vibrational Relaxation," *Physics of Fluids*, Vol. 5, No. 9, 1962, pp. 1022–1026.

[3]Marrone, P., "Inviscid Nonequilibrium Flow Behind Bow and Normal Shock Waves, Part I. General Analysis and Numerical Examples," Cornell Aeronautical Lab., Tech. Rept. QM-1626-A-12(I), Buffalo, NY, May 1963.

[4]Park, C., *Nonequilibrium Hypersonic Aerothermodynamcis*, Wiley, New York, 1990, p. 114.

[5]Park, C., "Assessment of Two-Temperature Kinetic Model for Ionizing Air," AIAA Paper 87-1574, 1987.

[6]Furudate, M., Nonaka, S., and Sawada, K., "Behavior of Two-Temperature Model in Intermediate Hypersonic Regime," *Journal of Thermophysics and Heat Transfer*, Vol. 13, No. 4, 1999, pp. 424–430.

[7]Josyula, E., and Bailey, W. F., "Vibration-Dissociation Coupling Using Master Equations in Nonequilibrium Hypersonic Blunt-Body Flow," *Journal of Thermophysics and Heat Transfer*, Vol. 15, No. 2, 2001, pp. 157–167.

[8]Josyula, E., and Bailey, W., "The Physics of Vibration-Dissociation Coupling in Hypersonic Flows," AIAA Paper 2001-2733, June 2001.

[9]Landau, L., and Teller, E., "Zur Theorie der Schalldispersion," *Physikalische Zeitschrift der Sowjetunion*, Vol. 10, No. 1, 1936, pp. 34–43.

[10]Huber, K., and Herzberg, G., *Constants of Diatomic Molecules*, Reinhold, New York, 1979.

[11]Park, C., "On Convergence of Computation of Chemically Reacting Flows," AIAA Paper 85-0247, Jan. 1985.

[12]Osipov, A. I., and Stupochenko, E., "Kinetics of the Thermal Dissociation of Diatomic Molecules I. Small Impurity of Diatomic Molecules in a Monoatomic Inert Gas," *Combustion, Explosion and Shock Waves*, Vol. 10, No. 3, 1974, pp. 303–313.

[13]Josyula, E., "Computational Study of Vibrationally Relaxing Gas past Blunt Body in Hypersonic Flows," *Journal of Thermophysics and Heat Transfer*, Vol. 14, No. 1, 2000, pp. 18–26.

[14]Josyula, E., "Oxygen Atoms' Effect on Vibrational Relaxation of Nitrogen in Blunt-Body Flows," *Journal of Thermophysics and Heat Transfer*, Vol. 15, No. 1, 2001, pp. 106–115.

R. P. Lucht
Associate Editor